Cross sections for one-electron capture by highly stripped ions of B, C, N, O, F, Ne, and S from He below 1 keV/amu

T. Iwai,* Y. Kaneko,† M. Kimura,‡ N. Kobayashi,† S. Ohtani, K. Okuno,†
S. Takagi,§ H. Tawara,|| and S. Tsurubuchi,**
Institute of Plasma Physics, Nagoya University, Nagoya 464, Japan
(Received 31 August 1981)

Cross sections for one-electron transfer from a He atom into the fully stripped, hydrogenlike, heliumlike, and lithiumlike B^{q+}, C^{q+}, N^{q+}, O^{q+}, F^{q+}, Ne^{q+} ions, and also highly stripped S^{q+} ions have been measured at the energy range of $1.5q-3.0q$ keV. The measured cross sections are nearly independent of the collision energy with a few exceptions, and most of the cross sections measured are about $(1\sim 4)\times 10^{-15}$ cm^2, but the cross sections for B^{4+}, C^{4+}, and N^{4+} ions are very small in the energy range studied. When the cross sections measured are plotted as a function of the ionic charge q of isoelectronic projectile ions, strong oscillations in the cross sections are observed. As a first approximation, this oscillatory behavior can be explained in terms of the classical one-electron model.

I. INTRODUCTION

The electron capture process by highly stripped ions is currently of great importance not only in basic atomic collision physics but also in such diverse fields as controlled-thermonuclear-fusion research, developments of x-ray laser devices and astrophysics.

In particular, the electron-capture process by highly stripped ions A^{q+} from atomic hydrogen at low energies,

$$A^{q+}+\mathrm{H}\rightarrow A^{(q-1)+}+\mathrm{H}^{+}\ , \qquad (1)$$

plays a key role in the energy and particle losses from high-temperature plasmas.[1] Because of a simple situation in the collision process of the fully stripped ion, a number of theoretical calculations have been reported.[2] On the other hand, it is difficult to obtain highly stripped ions at low energies and, therefore, experimental results are scarce for the fully stripped ions.[3] Until now, theoretical and experimental works including partially stripped ions have been concentrated on investigations of the dependence of the cross sections on the ionic charge q of the projectile ion and its nuclear charge Z_1 and on the collision energy.

Most of the theories are based on the concept of the quasimolecule $(A\text{-H})^{q+}$ during collisions. Then, the cross sections are mainly determined by interactions at the crossings between the diabatic potential curves of the initial $(A^{q+}\text{-H})$ and the final $(A^{(q-1)+}\text{-H}^{+})$ states. For the high-charge states of projectile ions, there are many curve crossings and it is possible to model the collision processes. These theories predicted that the cross sections change monotonically with the ionic charge q and are proportional to q^{α}, where α is equal to $1\sim 2$ dependently on the model used, and that the cross sections are nearly independent of the collision velocity at low and intermediate velocities $(10^6\sim 10^8$ cm/s). Meanwhile, for the low-q states, several theories showed that the cross sections do not scale according to such a simple rule as q changes. Aside from detailed calculations for the specified collision processes, Ryufuku, Sasaki, and Watanabe (RSW)[4] predicted a strongly oscillatory dependence of the cross sections on certain effective charges of projectile ions at low and intermediate energies (<10 keV/amu) using a model in which the projectiles are replaced by bare nuclei having the effective charges. They also showed the oscillation disappears at higher energies.

Experimental aspects including target atoms other than atomic hydrogen have been reviewed by Salzborn and Müller.[5] Most of the data have been obtained for partially stripped ions at energies higher than a few keV/amu. Almost all the experimental data show the monotonic dependence of the cross sections on q. However, there are experimental evidences that in some collisions cross sections do not change monotonically, but some bumps or dips exist. As for the H target atom, for example, Crandall et al.[6,7] and Gardner et al.[8] reported that the cross sections for C, N, O, F, and Xe ions show significant bumps at $q=3$ and 5 in the keV/amu energy region; Phaneuf reported very recently that the cross sections for C ions show neither monotonic change with q nor uniform velocity dependence below 500 eV/amu.[9] Recently, Bliman et al.[10] reported the nonmonotonic variation of the cross sections for C, N, O, and Ar ions incident on D_2 and Ar gas targets in the energy range of $1q \sim 10q$ keV. They concluded that such an oscillatory behavior of the cross sections is not due to the presence of metastable projectile ions but due to the electronic structure of the ions. Similar oscillations were observed by Cocke et al.[11] Mann et al.[12] also reported that the cross sections for the one-electron capture by highly stripped heavy ions change drastically in the magnitude with the ionization potential of the target atoms.

The helium atom, among others, is an interesting target atom, because its electronic structure is simple enough to treat theoretically, and because it is easily prepared as a target atom in collision experiments. The electron-capture process by highly stripped ions from He atom has been studied experimentally by several authors[13–19]. Zwally et al.[15,16] measured the cross sections of one-electron capture for C^{4+} and B^{3+} ions in the wide energy range of $0.3 \sim 40$ keV. Crandall[18] and Gardner et al.[19] measured the cross sections of one-electron capture for the He-like and the Li-like ions such as B^{q+}, C^{q+}, N^{q+}, and O^{q+} ions in the energy range of $6q \sim 23q$ keV, and observed the nonmonotonic variation with the charge state q. They also measured the cross section of two-electron capture and found that this cross section becomes greater than that of one-electron capture for the C^{4+} ion as the collision energy is reduced. No measurement of the cross sections, however, was reported for fully stripped ions or the H-like ions except for B^{4+} at low energies.[20]

The present paper describes our effort in measuring the cross sections of one-electron capture for highly stripped B, C, N, O, F, Ne, and S ions including the fully stripped ions in collision with helium target,

$$A^{q+} + \mathrm{He} \rightarrow A^{(q-1)+} + (\text{product}) \qquad (2)$$

at the collision energies below $3.0q$ keV. This is, to our knowledge, the first systematic measurement of the one-electron-capture cross section for highly stripped ions with the isoelectronic sequence.

II. EXPERIMENTAL TECHNIQUE

A. Ion source and experimental setup

The ion source in the present work, called NICE-1, is an electron-beam-ion source (EBIS) originally developed by Donets.[21] The ions are produced by a high-density electron beam confined by a strong magnetic field applied along the electron-beam axis.

The NICE-1 has a superconducting magnet (SCM) for generating a strong and stable magnetic field; the solenoid made of Nb-Ti is 100 cm in length and 10 cm in inside diameter (i.d.); the magnetic field can be varied up to 2 T; a persistent current-mode operation is chosen. A surface of the liquid-helium reservoir for the SCM works as a cryogenic pump to reduce the background gas pressure in the ionization region. An electron beam is extracted from a thoriated tungsten hair-pin-type gun and passes through an anode hole of 2 mm in radius and the subsequent 14 pieces of drift tubes of 3 cm in i.d. surrounded by the liquid-helium reservoir. A very small amount of gases is injected through a gap between the first and second drift tubes. Ions produced by electron impacts are trapped radially by the space-charge potential of the electron beam and axially by the potential barriers applied to the drift tubes. The step-by-step ionization of the trapped ions proceeds by successive electron bombardments. The diameter of the electron beam was not measured directly, but is estimated to be less than 0.5 mm. After passing through the drift tubes, the electron beam is received by an electron collector shielded from the magnetic field by a soft-iron plate and a μ-metal cylinder. A typical electron current is 15 mA at 2 kV and 1.2 T. The background gas pressure measured at the vacuum vessel of the NICE-1 is usually 2×10^{-10} Torr. Then the residual gas pressure in the ionization region is expected to be much less than 1×10^{-10} Torr. Such an ultrahigh vacuum is essentially important for producing the fully stripped ions. For the fully stripped C^{6+}, N^{7+}, and O^{8+} ions, stable isotope gases ^{13}CO, $^{15}N_2$, and $^{18}O_2$ are used to separate from impurity ions having $M/q=2$. BF_3, Ne, and SF_6 gases are used for B, Ne, F, and S ions.

The present experimental setup is schematically shown in Fig. 1. Ions extracted from the source are accelerated to a desired energy. An ion beam, formed after passing through an einzel lens and a pair of quadrupole lenses, is mass analyzed with a

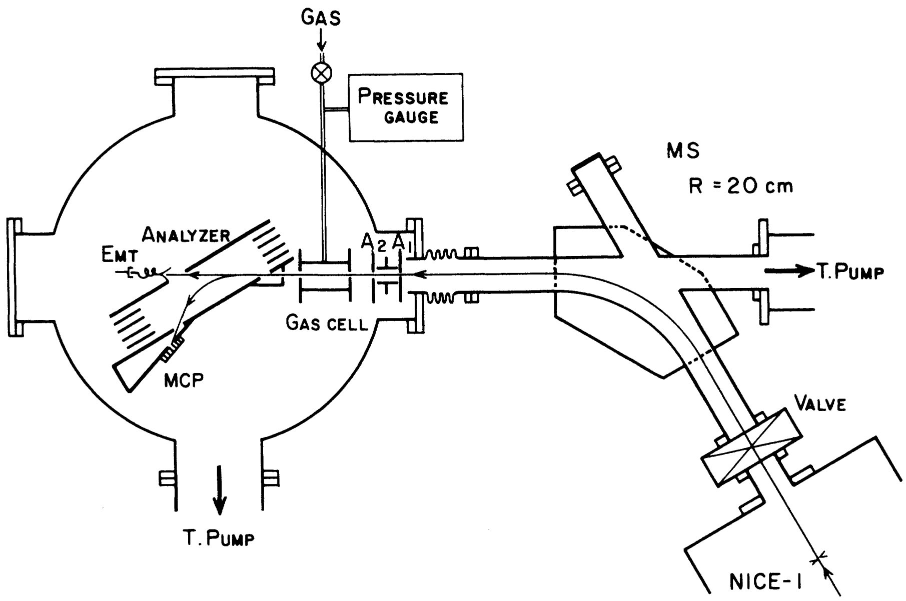

FIG. 1. Schematic view of the apparatus.

60° sector of 20-cm radius and injected into a collision cell. The ion beam is well collimated by a pair of beam-defining apertures of 1 mm diam A_1 and A_2; the distance between A_1 and A_2 is 5 cm and A_2 is placed 4 cm in front of the gas cell. The gas cell is 2 cm in length and its entrance and exit apertures are 0.8 and 1 mm in diameter, respectively. Ions which pass through the cell are charge separated with a parallel plate electrostatic analyzer located 1 cm behind the cell; the entrance and exit apertures of the analyzer plate are 5 mm in width and 8 mm in height. By changing the voltage applied to the analyzer, both the primary A^{q+} ions and the charge-changed $A^{(q-1)+}$ ions are detected with the same microchannel plate detector (MCP, HTV F1158) in a single-counting mode. Another detector, a continuous electron multiplier (EMT), aligned to the ion-beam axis, is used to identify the charge and mass of the primary ion. In order to reduce background signals, the pressure outside the collision cell is kept below 2×10^{-8} Torr with a 500-1/s turbomolecular pump. Figure 2 shows a typical charge-state spectrum of ^{15}N at the acceleration voltage of 2.5 kV. In contrast to the ordinary EBIS operation,[21] the NICE-1 is operated in a mode where gas atoms to be ionized and the electron beam are continuously supplied.[22] Therefore the charge of ions produced is widely distributed over from $q=1$ to 7 for N ions; their distribution is strongly dependent on the gas pressure in the ion source and the electron energy. The intensity of the fully stripped N^{7+} ions shown in Fig. 2 is typically 2×10^3 counts per s (cps). Because of such a wide charge distribution, ions with different charge state are obtained without changing the ion source parameters.

The He target gas is introduced through a stainless-steel tubing from a cylinder containing He of high purity (99.999%). In order to avoid any contamination with impurities, the tubing is carefully connected and preheated.

B. Measurement of cross sections

1. Determination of cross sections

Cross section for the one-electron-capture process $\sigma_{q,q-1}$ is determined by

$$\sigma_{q,q-1}=\frac{\alpha_q S_{q-1}}{\alpha_{q-1} S_q N L}\ , \tag{3}$$

where S_q is the count rate for the primary A^{q+} ions, S_{q-1} for the charge-changed $A^{(q-1)+}$ ions, N the number density of the target He atom, L the collision-path length, and α_q and α_{q-1} are the detection efficiencies for the A^{q+} and $A^{(q-1)+}$ ions. In the present detection system, we assumed that the detection efficiency of the MCP is identical for all the ions with different charge states, that is,

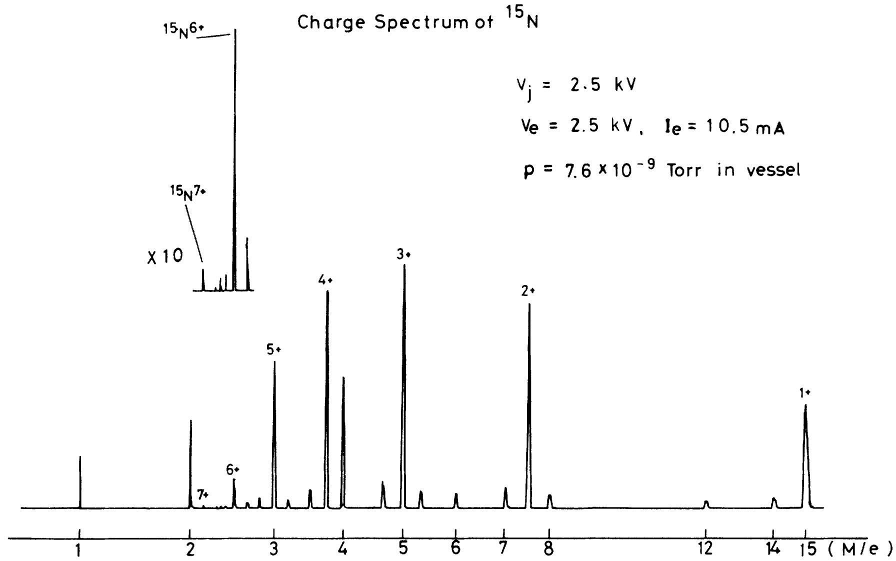

FIG. 2. Typical spectrum of the charge-state distribution of $^{15}N^{q+}$ ions extracted at 2.5 kV from the NICE-1 under the condition that the electron beam intensity is 10.5 mA at 2.5 kV. Ion detection is made by the EMT shown in Fig. 1.

$\alpha_q = \alpha_{q-1}$, because the ion impact energy on the MCP is always higher than a few keV where the coefficient of the secondary electron emission is usually larger than unity.

It is found that the pulse-height distribution from the MCP used is nearly independent of the ion impact energy for all the charge states, but dependent on the charge state and the count rate. The maximum of the pulse-height distribution shifts towards higher values as the charge state increases, and the pulse-height distribution becomes broader and its maximum shifts towards lower values as the count rate increases. Therefore, for each experimental run, care is taken to minimize the counting loss due to reduction of the pulse height by monitoring the pulse-height distribution from the MCP with a multichannel pulse-height analyzer and an oscilloscope. The count rate of the primary ion beam is always kept less than 5×10^3 cps. Spacial detection efficiency of the MCP used is checked by varying the analyzer voltage, and is confirmed to be fairly uniform over the detection area within the limits of stabilities of incident ion beams.

The target density N in the gas cell is determined by the use of the calculated conductance of the capillary tube and cell apertures and by measurements of the pressure in the He gas reservoir with a capacitance manometer (BAROCELL). Details of the determination have been described in Ref. 23. The collision-path length L is assumed to be the distance between the apertures of the cell which is 2 cm.

Actually, cross sections for the one-electron-capture process are determined through the initial growth of the charge-changed $A^{(q-1)+}$ ions. This procedure is illustrated in Fig. 3 as an example, which shows the count rate for the primary N^{7+} ions and charge-changed N^{6+} ions as a function of the target thickness NL. At first, the analyzer voltage is set for the primary ions to impact on the MCP while the collision cell is evacuated, and then

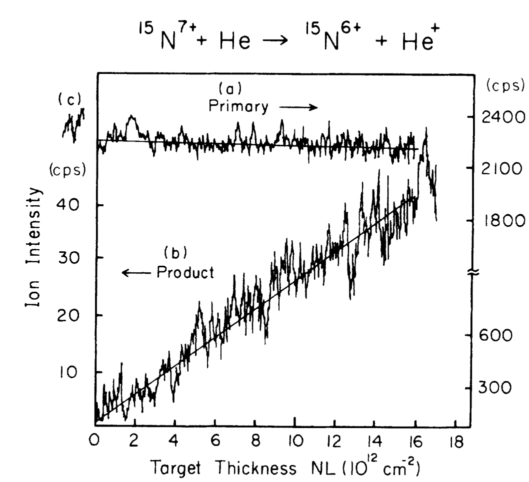

FIG. 3. Growth-rate curve of the charge-changed N^{6+} ion for the primary N^{7+} ion. See text for detail.

the target He gas is introduced into the cell until a few % reduction of the count rate of the primary ions is observed [part (a) in Fig. 3]. Secondly, the analyzer voltage is set for the charge-changed ions and the target gas pressure is reduced continuously [part (b) in Fig. 3]. Finally, the analyzer voltage is returned for the primary ions in order to check the reproducibility of the count rate of the primary ions [part (c) in Fig. 3]. Then the cross section can be determined from the slope of the growth-rate curve. This procedure has four advantages at least. First, it is easy and sure to check for single-collision conditions, which are necessary to apply Eq. (3), by directly observing the linearity of the growth-rate curve. Second, background noise signals are readily subtracted from the count rate of the charge-changed ions S_{q-1} which is usually several tens cps when S_q is of the order of 10^3 cps. Third, it is very useful to reduce statistical errors, because the continuous variation of the target thickness corresponds to average out a lot of point-to-point measurements. Fourth, the identification of the primary ions, which is usually not so easy because of the presence of impurity ions in the primary beam, can be reconfirmed by the analyzer potentials to be applied for the A^{q+} and $A^{(q-1)+}$ ions.

2. *Uncertainties*

Most of uncertainties come from the stability of the primary ion beam, determination of the slope of the growth-rate curve and of the target thickness. The uncertainty in the stability of the primary ion beam is estimated to be less than $\pm 8\%$. The uncertainty associated with determination of the slope of the growth-rate curve is less than $\pm 20\%$. Determination of the target thickness involves about $\pm 10\%$ uncertainty as estimated in the previous work.[23] Further uncertainty arises from the dependence of counting efficiency of the detector on the ionic charge state and count rate. This uncertainty, however, is elaborately reduced as mentioned in Sec. II B, and estimated at $\pm 5\%$. The total uncertainty for the absolute value of the cross section therefore is estimated to be about $\pm 30\%$ in quadrature sum except for the uncertainty in the primary ion-beam purity. All ions studied are completely separated and well identified by the use of stable isotopes. However, we cannot say whether the primary ions are extracted in their ground state although it is said that an EBIS-type ion source produces few ions in the metastable states.[24]

III. RESULTS AND DISCUSSION

A. General results and comparison with others

Table I presents the measured cross sections for the one-electron capture by highly stripped B, C, N, O, F, Ne, and S ions together with total uncertainties. In general, most of the cross sections measured are about $1\sim 4\times 10^{-15}$ cm^2 in the collision energy range of $1.5q\sim 3.0q$ keV investigated in the present work. However, it is quite remarkable that the cross sections obtained for B^{4+}, C^{4+}, and N^{4+} ions are anomalously small. The measured cross sections are nearly independent of the collision energy, though the present energy range is rather narrow. Some cross sections, however, increase with the collision energy in such collisions as B^{4+}-, C^{3+}-, F^{8+}-, Ne^{8+}-, and S^{13+}-He systems.

There are several groups which have studied experimentally the A^{q+}-He system. All of the present data are illustrated in Figs. 4(a)–4(g) for comparison with others. Owing to the different energy range studied, the present data cannot be compared directly to others except for the data of Zwally *et al.* Nikolaev *et al.*[14] reported the cross sections $\sigma_{q,q-1}$ for the fully stripped B^{5+} ion, the H-like B^{4+} and N^{6+} ions, the He-like B^{3+}, C^{4+}, N^{5+}, and O^{6+} ions, and the Li-like B^{2+}, C^{3+}, N^{4+}, and O^{5+} ions. Their data, however, were obtained in the energy range about 100 times as high as the present ones; in their energy range $\sigma_{q,q-1}$ sharply decreases with the collision energy; their data are not shown in Fig. 4. Crandall[18] and Gardner *et al.*[19] obtained their data at energies a few times as high as the present ones. In their energy range, most of the cross sections are nearly independent of energy. As seen in Figs. 4(a)–4(d), rough extrapolation of their data indicates that the present data seem to be in fairly good agreement with theirs for the $B^{3,4+}$, $C^{3,4+}$, $N^{4,5+}$, and $O^{5,6+}$ ions which are the only ionic species available for comparison. Data of Zwally and Koopman[15] for the C^{4+} ion and of Zwally and Cable[16] for the B^{3+} ion, which can be directly compared with ours, are in good agreement with the present data as seen in Figs. 4(a) and 4(b). As for the fully stripped C^{6+}, N^{7+}, and O^{8+} ions, the present data are compared with the results of Afrosimov *et al.*[20] Though the collision energy range tested is different, both data seem to be smoothly connected with each other.

It is found from the present data that the cross sections $\sigma_{q,q-1}$ vary with the ionic charge q drastically and also with nuclear charge Z_1 of projectile

TABLE I. One-electron-capture cross sections $\sigma_{q,q-1}$ for the highly stripped ion from He at collision energy E.

Ion	E (keV/amu)	$\sigma_{q,q-1}$ (10^{-16} cm^2)
B^{3+}	0.44	12.2 ±2.4
	0.55	17.3 ±3.5
	0.68	13.2 ±2.6
	0.82	14.6 ±2.9
B^{4+}	0.58	0.92±0.28
	0.73	1.36±0.41
	0.91	1.53±0.47
	1.09	2.87±0.86
B^{5+}	0.73	8.4 ±1.7
	0.91	8.3 ±1.7
	1.14	11.6 ±2.3
	1.36	9.2 ±1.8
C^{3+}	0.38	14.7 ±2.9
	0.50	18.8 ±2.9
	0.63	22.5 ±4.5
C^{4+}	0.50	0.85±0.26
	0.67	1.72±0.52
	0.83	1.16±0.35
C^{5+}	0.63	15.2 ±3.0
	0.83	14.8 ±3.0
	1.04	14.2 ±2.8
$^{13}C^{6+}$	0.69	9.0 ±1.8
	0.92	7.9 ±1.6
	1.15	13.2 ±2.6
N^{4+}	0.43	3.0 ±0.9
	0.57	3.7 ±1.1
	0.71	3.5 ±1.1
N^{5+}	0.54	13.4 ±2.7
	0.71	16.8 ±3.4
	0.89	14.4 ±2.9
$^{15}N^{6+}$	0.68	14.2 ±2.8
	0.80	15.5 ±3.1
	1.00	15.0 ±3.0
$^{15}N^{7+}$	0.78	10.5 ±2.1
	0.93	10.9 ±2.2
	1.17	11.9 ±2.4
O^{5+}	0.47	22.7 ±4.5
	0.63	25.1 ±5.0
	0.78	23.9 ±4.8
O^{6+}	0.56	9.0 ±1.8
	0.75	11.6 ±2.3
	0.94	12.1 ±2.4
$^{18}O^{7+}$	0.58	12.3 ±2.5
$^{16}O^{7+}$	0.66	13.6 ±2.7
	0.88	12.8 ±2.6
	1.09	14.6 ±2.9
$^{18}O^{8+}$	0.76	27.3 ±5.5
	0.89	30.6 ±6.1
	1.11	34.4 ±6.9
F^{6+}	0.54	18.5 ±3.7
	0.63	18.8 ±3.8
	0.79	19.4 ±3.9
F^{7+}	0.63	16.2 ±3.2
	0.74	17.6 ±3.5
	0.92	21.7 ±4.3
F^{8+}	0.72	26.7 ±5.3
	0.84	30.4 ±6.1
	1.05	34.5 ±6.9
$^{20}Ne^{7+}$	0.53	30.4 ±6.1
$^{22}Ne^{7+}$	0.64	30.4 ±6.1
	0.80	32.2 ±6.4
$^{20}Ne^{8+}$	0.60	28.0 ±5.6
$^{22}Ne^{8+}$	0.73	30.6 ±6.1
	0.91	33.9 ±6.8
$^{20}Ne^{9+}$	0.77	18.1 ±3.6
	0.90	20.1 ±4.0
	1.13	19.3 ±3.9
S^{11+}	0.58	40.2 ±8.0
	0.69	37.7 ±7.5
	0.86	37.5 ±7.5
S^{13+}	0.69	44.8 ±9.0
	0.81	45.3 ±9.1
	1.02	50.5 ±10.1

ions at the present energy range. The variation of the cross sections is enhanced for highly stripped low-Z_1 ions and is not simple and monotonic as q changes, but really depends on both q and Z_1.

B. Ionic charge dependence

In Fig. 5 are shown the cross sections reasonably interpolated at 0.8 keV/amu as a function of the initial charge state q for all ions investigated. The lines are drawn to connect data for ions having the same isoelectronic sequences such as fully stripped, H-like, He-like, and Li-like ions. As seen in Fig. 5, the cross sections oscillate strongly with q for all ions. These oscillations are particularly significant at low q. For example, the cross sections for $q=3$ and 5 are almost one order of magnitude larger than those for $q=4$. Furthermore, for the same q, the cross sections depend on the atomic number Z_1 of the projectile ions. These oscillations with q and variations with Z_1 tend to disappear with increasing q and Z_1. In fact, when the oscillation of the measured cross sections in the present work is smoothed out, the q dependence is quite similar to that obtained from an empirical formula of Müller and Salzborn,[25] which is shown as a dotted line in Fig. 5.

C. Classical one-electron model with effective charge

Few theoretical studies have been made on the electron-capture process for A^{q+}-He collisions.

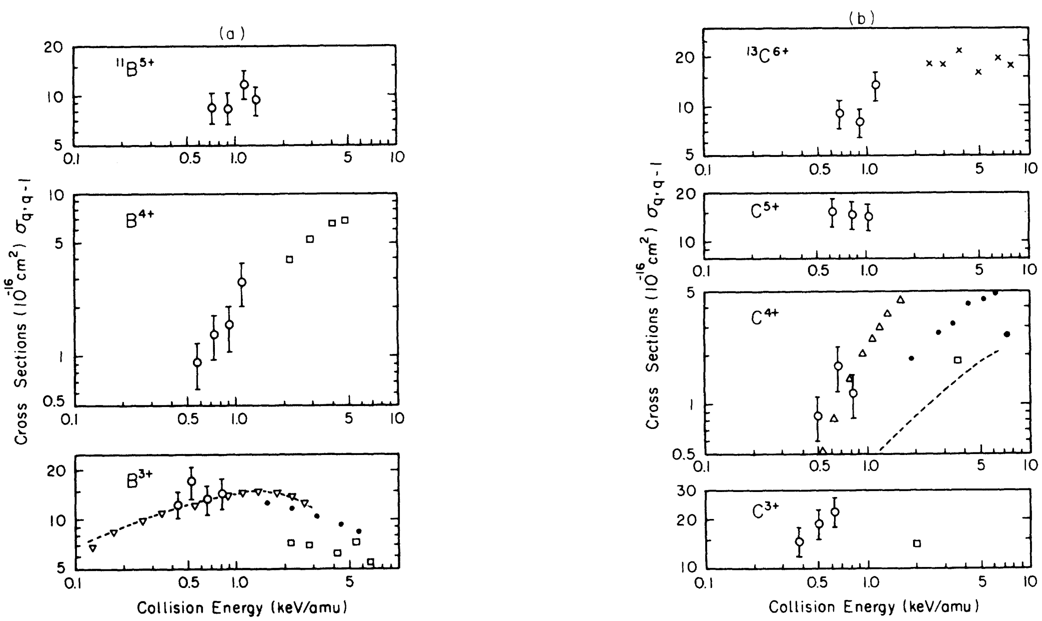

FIG. 4. (a) Cross section of one-electron capture by B^{3+}, B^{4+}, and B^{5+} ions incident on He. Open circles are the present data, triangles the data of Zwally and Cable (Ref. 16), solid circles the data of Crandall (Ref. 18), squares the data of Gardner *et al.* (Ref. 19). Dashed line is the theoretical result of Shipsey *et al.* (Ref. 26). (b) Cross sections of one-electron capture by C^{3+}, C^{4+}, C^{5+}, and C^{6+} ions incident on He. Open circles are the present data, triangles the data of Zwally and Koopman (Ref. 15), solid circles the data of Crandall (Ref. 18), squares the data of Gardner *et al.* (Ref. 19), crosses the data of Afrosimov *et al.* (Ref. 20). Dashed line is the theoretical result of Shipsey *et al.* (Ref. 26). (c) Cross sections of one-electron capture by N^{4+}, N^{5+}, N^{6+}, and N^{7+} ions incident on He. Open circles are the present data, solid circles the data of Crandall (Ref. 18), squares the data of Gardner *et al.* (Ref. 19), crosses the data of Afrosimov *et al.* (Ref. 20). (d) Cross sections of one-electron capture by O^{5+}, O^{6+}, O^{7+}, and O^{8+} ions incident on He. Open circles are the present data, solid circles the data of Crandall (Ref. 18), squares the data of Gardner *et al.* (Ref. 19), crosses the data of Afrosimov *et al.* (Ref. 20). (e) Cross sections of one-electron capture by F^{6+}, F^{7+}, and F^{8+} ions incident on He. (f) Cross sections of one-electron capture by Ne^{7+}, Ne^{8+}, and Ne^{9+} ions incident on He. (g) Cross sections of one-electron capture by S^{11+} and S^{13+} ions incident on He.

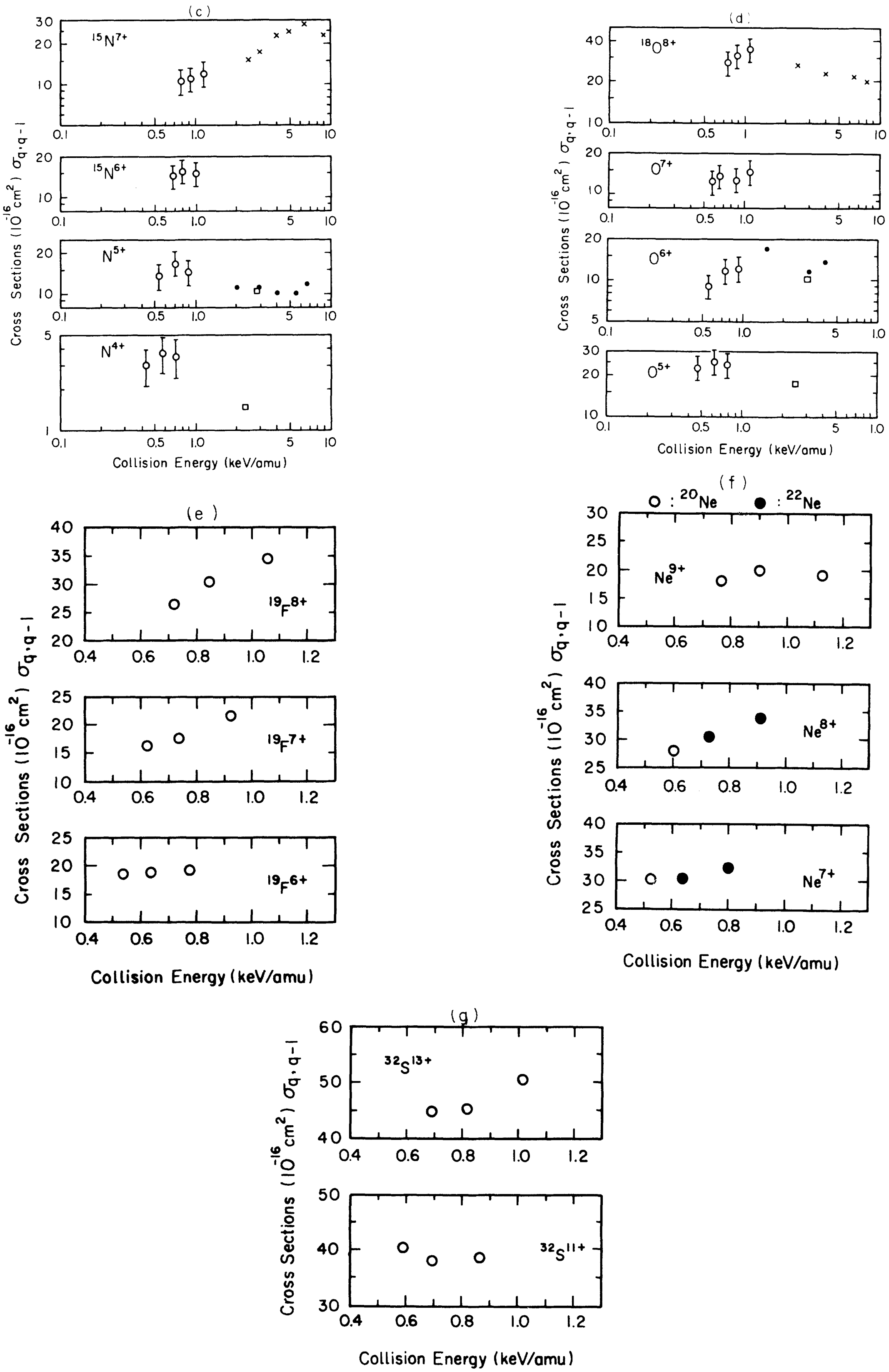

FIG. 4. (*Continued*.)

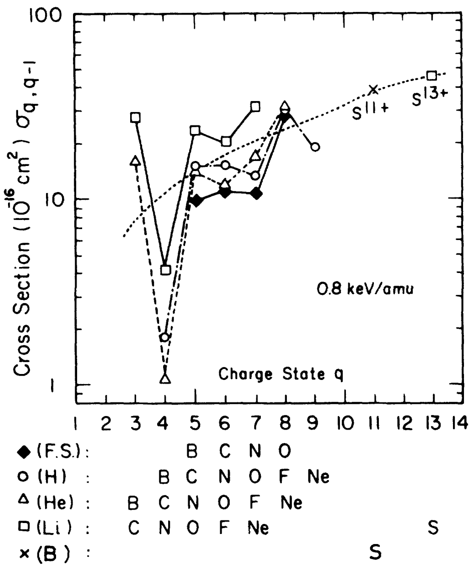

FIG. 5. Measured cross sections $\sigma_{q,q-1}$ at 0.8 keV/amu as a function of the ionic charge q of projectile ions. The dotted line is obtained from the empirical formula of Müller and Salzborn (Ref. 25).

Shipsey *et al.*[26] calculated the cross sections for B^{3+}- and C^{4+}-He collisions by the use of the molecular-orbital method, and their results for the one-electron-capture process are shown as dashed lines in Figs. 4(a) and 4(b). Their results agree with the present data and those of Zwally and Cable[16] for B^{3+} ions, but their cross sections are somewhat smaller than the experimental results for C^{4+} ions. Except for their calculations, there has been neither detailed calculation of individual collision processes nor overall treatment for better understanding of the A^{q+}-He collision systems systematically.

As mentioned in Sec. I, similar oscillations of the cross sections were predicted by RSW[4] as a function of the effective charge of projectiles for the A^{q+}-H collisions. Their calculation is based upon the unitarized-distorted-wave approximation[27] (UDWA), but they also showed that the UDWA treatment becomes equivalent to the classical treatment at low energies. Hence, as a first approximation, we adopt a classical one-electron model in the sense of RSW in order to understand the oscillation phenomena observed in the present work.

In the classical one-electron model, the projectile ions are replaced by bare nuclei having the effective charge Z_1^* and the He atom is replaced by the system of a bare nucleus having the effective charge Z_2^* plus one electron which is to be transferred into the projectile ion. Such a bare nucleus plus one-electron system behaves hydrogenically, that is, its energy level is given by $-(Z^*)^2/2n^2$, where n is the principal quantum number of the level concerned. The effective charge Z^* is determined from the ionization potential I_g of the ground state (n_g) of the system

$$Z^* = n_g (I_g / I_{\rm H})^{1/2} , \tag{4}$$

where $I_{\rm H}$ is the ionization potential of the H atom. As the ionization potential I_g, empirical values of Lotz[28] are used. Then, the energy level of the excited state (n) is calculated by

$$\frac{-(Z^*)^2}{2n^2} = \frac{-I_g n_g^2}{(2n^2 I_{\rm H})} . \tag{5}$$

According to the classical one-electron model, the electron transfer from He atom to projectile ions occurs when the energy levels of the collision system before and after collision coincide diabatically with each other, that is, the quasiresonance condition is fulfilled:

$$\frac{-Z_1^*}{R} - \frac{(Z_2^*)^2}{2n_2^2} = \frac{-(Z_1^*)^2}{2n_1^2} - \frac{Z_2^*}{R} , \tag{6}$$

where R is the internuclear distance between projectile ion and the target He atom. The left-hand side of Eq. (6) corresponds to the diabatic potential energy of the n_2 state of the target He atom perturbed by the Coulomb potential of the projectile ion before collision, and the right-hand side of Eq. (6) does to that of the n_1 state of the projectile ion plus one electron perturbed by the Coulomb potential of the He^+ ion after collision. In the present case, $n_2 = 1$ since the electron is in the ground state of the He atom.

The solution R in Eq. (6) gives the crossing point of the two diabatic potential curves. There are many possible crossing points corresponding to many different n_1 states into which the electron is to be transferred. According to the classical model, however, the electron transfer becomes possible when the diabatic potential energy before collision exceeds the maximum value of the potential barrier $-V_m$ formed between the projectile ion and the target atom:

$$\frac{-Z_1^*}{R} - \frac{(Z_2^*)^2}{2n_2^2} \geq -V_m \tag{7}$$

and

$$V_m = [(Z_1^*)^{1/2} + (Z_2^*)^{1/2}]^2 / R . \tag{8}$$

From Eqs. (6) and (7), the integer n corresponding to the state where the electron can be transferred is determined as follows:

$$n \leq n_1 , \tag{9}$$

where

$$n_1 = \left[\frac{Z_1^*}{Z_2^*} \right] \left[\frac{[Z_2^* + 2(Z_1^* Z_2^*)^{1/2}]}{[Z_1^* + 2(Z_1^* Z_2^*)^{1/2}]} \right]^{1/2} . \tag{10}$$

Then the distance R_n where one-electron transfer takes place is given by

$$R_n = \frac{(Z_1^* - Z_2^*)}{[(Z_1^*)^2/2n^2 - (Z_2^*)^2/2n_2^2]} . \tag{11}$$

Assuming the probability of one-electron transfer to be $\frac{1}{2}$, the classical cross section $\sigma_{q,q-1}$ is given as

$$\sigma_{q,q-1} = (\tfrac{1}{2})\pi R_n^2 . \tag{12}$$

D. Comparison between the measured cross sections and the classical model

Figure 6 shows the measured cross sections at 0.8 keV/amu plotted as a function of the effective charge Z_1^* derived from Eq. (4) together with those calculated from Eq. (12) based on the classical one-electron model (dotted curve). The number of n in

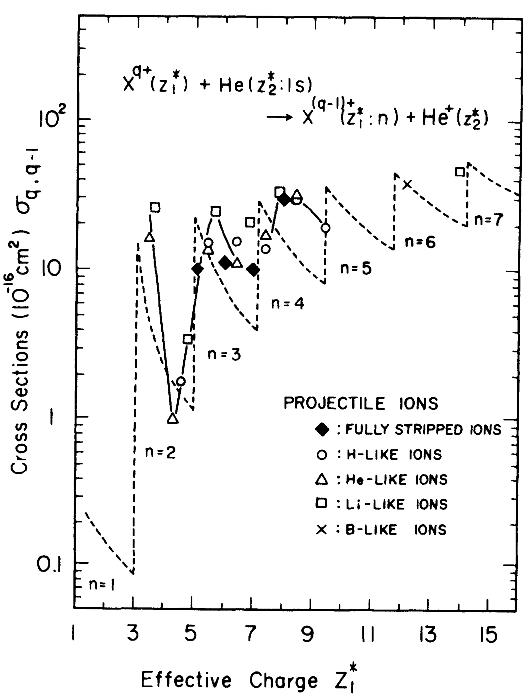

FIG. 6. Comparison of the measured cross sections at 0.8 keV/amu with the cross sections calculated in terms of the classical one-electron model shown as the dotted curve. Cross sections are plotted as a function of the effective charge Z_1^* of projectile ions.

Fig. 6 represents the principal quantum number of the level of the ion (projectile plus one electron) into which the electron is captured. It is noted that almost all the measured cross sections come together on a single curve. The oscillation is enhanced for low-Z_1^* ions and tends to vanish for high-Z_1^* ions. This oscillatory behavior is similar to the calculated one, though the agreement in the phase of the oscillation is not so good. Since the present calculation based on the classical model is very crude, the poor agreement between the calculation and the experimental results is not surprising. The discrepancy is partly due to neglect of the tunnel effect, neglect of the polarization effect, and so on.

In essence, however, the oscillatory behavior of the cross sections observed in the present work is a good indication that in highly stripped ion collisions at low energies, the electron is captured selectively into the level with a particular quantum number n in the collision system. The observed oscillation is significant for low-Z_1^* ions. For low-Z_1^* ions, the energy level into which the electron is transferred has a small value of n, and then its adjacent levels are largely separated. This causes a significant change in the cross section if the n value changes from n to $n+1$. On the other hand, for high-Z_1^* ions, the electron is captured into a level having a large n around which a number of energy levels are densely located. This gives rise to a minor change in the cross section if n is changed by one, and more than a single level may have a chance to capture one electron from the target atom. These should be reasons why the amplitude of the oscillation in the cross section tends to diminish towards higher-Z_1^* ions.

Such an oscillatory behavior should be dependent on the collision energy. The data of Gardner *et al.*,[19] which were obtained at energies a few times as high as the present energy range, show oscillations around $q=4$ for B^{q+}, C^{q+}, and N^{q+} ions, but the amplitude of their oscillation is smaller than the present one. The present classical model is essentially independent of energy. More sophisticated calculations would be desired.

ACKNOWLEDGMENTS

This work was carried out as a part of the Guest Research Program at the Institute of Plasma Physics, Nagoya University. The authors are grateful to Professor H. Kakihana, Director of the Institute, and to Emeritus Professor K. Takayama, the former Director of the Institute, for their encouragement throughout this work.

*Permanent address: Department of Liberal Arts, Kansai Medical University, Hirakata, Osaka 573, Japan.

†Permanent address: Department of Physics, Tokyo Metropolitan University, Setagaya-ku, Tokyo 158, Japan.

‡Permanent address: Department of Physics, Osaka University, Toyonaka, Osaka 560, Japan.

§Permanent address: Department of Electric Engineering, Doshisha University, Kyoto 602, Japan.

||Permanent address: Nuclear Engineering Department, Kyushu University, Fukuoka 812, Japan.

**Permanent address: Department of Applied Physics, Tokyo University of Agriculture and Technology, Koganei, Tokyo 184, Japan.

[1] *Atomic and Molecular Processes in Controlled Thermonuclear Fusion,* edited by M. P. C. McDowell (Plenum, New York, 1979).

[2] Progress in theories is summarized by R. E. Olson, in *Electronic and Atomic Collisions,* edited by N. Oda and K. Takayanagi (North-Holland, Amsterdam, 1980), p. 391.

[3] Experimental data up to the early 1980's including partially stripped ions are compiled by Y. Kaneko, T. Arikawa, Y. Itikawa, T. Iwai, T. Kato, M. Matsuzawa, Y. Nakai, K. Okuno, H. Ryufuku, H. Tawara, and T. Watanabe in Institute of Plasma Physics Report No. IPPJ-AM-15, Nagoya University, 1980 (unpublished).

[4] H. Ryufuku, K. Sasaki, and T. Watanabe, Phys. Rev. A 21, 745 (1980).

[5] E. Salzborn and A. Müller, Ref. 2, p. 407.

[6] D. H. Crandall, R. A. Phaneuf, and F. W. Meyer, Phys. Rev. A 19, 504 (1979).

[7] D. H. Crandall, R. A. Phaneuf, and F. W. Meyer, Phys. Rev. A 22, 379 (1980).

[8] L. D. Gardner, J. E. Bayfield, P. M. Koch, I. A. Sellin, D. J. Pegg, R. S. Peterson, and D. H. Crandall, Phys. Rev. A 21, 1397 (1980).

[9] R. A. Phaneuf, Phys. Rev. A 24, 1138 (1981).

[10] S. Bliman, J. Aubert, R. Geller, B. Jacquot, and D. van Houtte, Phys. Rev. A 23, 1703 (1981).

[11] C. L. Cocke, R. D. DuBoir, T. J. Gray, and E. Justiniano, IEEE Trans. Nucl. Sci. NS-28, 1032 (1981).

[12] R. Mann, F. Folkmann, and H. F. Beyer, J. Phys. B 14, 1161 (1981).

[13] C. W. Sherwin, Phys. Rev. 57, 814 (1940).

[14] V. S. Nikolaev, L. N. Fateeva, I. S. Dmitriev and Ya. A. Teplova, Zh. Eksp. Teor. Fiz. 40, 989 (1961) [Sov. Phys.—JETP 13, 659 (1961).

[15] H. J. Zwally and D. W. Koopman, Phys. Rev. A 2, 1851 (1970).

[16] H. J. Zwally and P. G. Cable, Phys. Rev. A 4, 2301 (1971).

[17] J. Goldhar, R. Mariella, Jr., and A. Javan, Appl. Phys. Lett. 29, 96 (1976).

[18] D. H. Crandall, Phys. Rev. A 16, 958 (1977).

[19] L. D. Gardner, J. E. Bayfield, P. M. Koch, I. A. Sellin, D. J. Pegg, R. S. Peterson, M. S. Mallory, and D. H. Crandall, Phys. Rev. A 20, 766 (1979).

[20] Very recently, preliminary reports appeared in the XII-ICPEAC, Gatlinburg, Tennessee, 1981: Data for fully stripped C, N, O, and Ne ions by Afrosimov *et al.,* in *Abstracts of the XII ICPEAC, Gatlinburg, Tennessee, 1981,* edited by S. Datz (North-Holland, Amsterdam, 1981), p. 690; data for C^{5+}, N^{6+}, $O^{7,8+}$, F^{8+}, and Ne^{9+} by our group in the papers, p. 696. A brief report of the present work except for B^{q+} ions is described by Kaneko *et al.* in *Physics of Electronic and Atomic Collisions,* edited by S. Datz (North-Holland, Amsterdam, 1982), p. 697.

[21] E. D. Donets, IEEE Trans. Nucl. Sci. NS-23, 897 (1976).

[22] H. Imamura, Y. Kaneko, T. Iwai, S. Ohtani, N. Kobayashi, K. Okuno, S. Tsurubuchi, M. Kimura, and H. Tawara, Nucl. Instrum. Methods. 188, 233 (1981).

[23] Y. Kaneko, T. Iwai, S. Ohtani, K. Okuno, N. Kobayashi, S. Tsurubuchi, M. Kimura, and H. Tawara, J. Phys. B 14, 881 (1981).

[24] H. Klinger, A. Müller, and E. Salzborn, J. Phys. B 8, 230 (1975).

[25] A. Müller and E. Salzborn, Phys. Lett. 62A, 391 (1977).

[26] E. J. Shipsey, J. C. Browne, and R. E. Olson, Phys. Rev. A 15, 2166 (1977).

[27] H. Ryufuku and T. Watanabe, Phys. Rev. A 19, 1538 (1979).

[28] W. Lotz, J. Opt. Soc. Am. 57, 873 (1967).